Synthesis of a novel core-shell-structure activated carbon material and its application in sulfamethoxazole adsorption
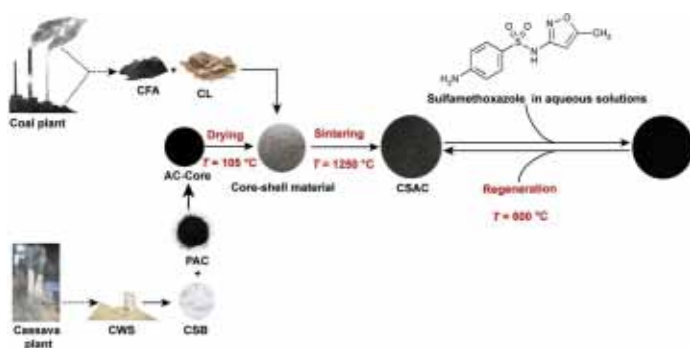
Pamphile Ndagijimana[a,b,1], Xuejiao Liu[a,b,1], Guangwei Yu[a,*], Yin Wang[a,*]

[a] *CAS Key Laboratory of Urban Pollutant Conversion, Institute of Urban Environment, Chinese Academy of Sciences, Xiamen, 361021, China*
[b] *University of Chinese Academy of Sciences, Beijing, 100049, China*

GRAPHICAL ABSTRACT

ARTICLE INFO

ABSTRACT

The increasing release of pharmaceutical and personal care products (PPCPs) into water poses serious threats to human beings. In this study, a novel core-shell activated carbon (CSAC) material with a high-mechanical-strength porous ceramic shell was synthesized and tested by adsorbing sulfamethoxazole (SMX) from aqueous solutions. An activated carbon core (AC core) was synthesized from a mixture of powder AC (92%) and cassava waste splinters binder (8%). Moreover, a shell with a high thickness of 0.13 cm and compressive strength (2.92 MPa) was generated from the mixture of coal fly ash and clay at ratio of 60:40. It demonstrated high protection of the AC core. The adsorption efficiency of SMX by CSAC attained 99.0% and 97.9% at initial concentrations of 5 and 10 mg L^{-1}, respectively. Furthermore, 77.0, 68.6 and 60.4% of SMX were adsorbed at higher concentrations of 30, 50, and 100 mg L^{-1}, respectively. The kinetics study demonstrated that the adsorption of SMX followed pseudo-second-order kinetics. Moreover, the sorption isotherm was better fitted to Freundlich isotherms. Finally, SMX adsorption on CSAC simultaneously depended on the pore texture of CSAC and the hydrophobic properties of SMX, as well as the π-π bonds and electrostatic interactions between them.

1. Introduction

The waste and effluent released from manufacturing industries into the environment have been exacerbating water pollution as the population continues to use manufactured products that contain chemicals such as antibiotics, aspirin, synthetic masks and other pharmaceuticals,

* Corresponding authors.
  E-mail addresses: gwyu@iue.ac.cn (Y. Guangwei), yinwang@iue.ac.cn (W. Yin).
  [1] Pamphile Ndagijimana and Xuejiao Liu contributed equally to this article.

and personal care products (PPCPs) [1,2]. The continuous discharge of PPCPs into the aquatic ecosystem is causing water pollution as emerging contaminants threatening the safety of drinking water and aquatic organisms. Moreover, it is difficult to completely remove PPCPs through conventional wastewater treatment plants (WWTPs) owing to their high polarity and solubility in water [3–5]. These properties facilitate the release of PPCPs from WWTPs, effluents, and urban wastewater that flow into surface, drinking, and ground water [6,7]. Antibiotics (a main component of PPCPs)-contaminated water and wastewater are a global environmental concern. Antibiotics have been found to be persistent in water due to their strong affinity for water, and they are not easily metabolized and absorbed by animals; eventually, will accumulate and create toxicity, posing an ecotoxicological danger to aquatic and terrestrial life [8,9]. For example, sulfamethoxazole (SMX) is an antibiotic that is not easily removed completely by WWTPs, especially its residues [10,11]. Exposure to this contaminant may cause adverse effects to humans, including hepatic cancer and alteration of genetic traits [12–14], and its environmental behavior is still unclear [15]. Therefore, it is vital to withdraw antibiotics from the aquatic ecosystem.

Multiple treatment techniques, namely oxidation, sedimentation, coagulation, flocculation, and filtration, were adopted to eliminate particulate matter (turbidity) and disease-producing microorganisms from water. However, most of these methods were not efficient to overcome the problem of antibiotics in water [16–18]. As reported previously, adsorption on solid particles plays a pivotal role in regulating the ecological effects of SMX [12]. This method has several advantages, including affordable operation and environmental sustainability [19]. Adsorbent bearing desired properties such as porous texture, surface charge, and hydrophobicity along with the solution's pH are commonly regarded as beneficial and most significant factors for SMX removal [20,21]. Owing to its excellent porous texture and rich surface chemistry, activated carbon (AC) is widely used to remove many different contaminants. Also, previous studies have shown that SMX in water can be removed by granulated activated carbon (GAC) or powdered activated carbon (PAC) owing to the amine groups or benzene rings in the structure of most SMX [12,22,23]. However, on one side the application of AC is limited by a decrease in pressure, regenerability, dusting, and attrition [24,25]. On the other side, the application of PAC is handicapped because of shortcoming recyclability from water or wastewater. The residual PAC in the liquid can even cause clogging and a pressure drops in the filtration system [26]. To some extent, the use of granular activated carbon (GAC) for the adsorption application would be a preferred option over PAC; however, the strength of GAC should be high enough to withstand the pressure when installed in the absorption column. Expectedly, novel strategies are necessary to address the existing challenges. Coal fly ash is an anthropogenic material susceptible to posing environmental hazards (water and soil pollution) if it is not properly disposed [27]. Cassava fibrous residue (CFR) is another constituent waste originated from milling process of cassava with environmental risk [28]. Interestingly, these splinters are typically cheaper and with high content of starch. Thus, they have a potential interest in application rather to create disposal concerns. Recently, a carbon core protected by inorganic membrane shell was prepared for suitability in heat transfer and enhancing the mechanical properties of a solid catalyst application, but could not be applied in adsorption in aqueous solution [29,30].

Therefore, in this study, we have been motivated by using originally waste materials to synthesize a novel CSAC material with a high-mechanical-strength porous ceramic shell to eliminate PPCPs in aquatic environment. The aims of this study were to (i) optimize the synthesis of CSAC samples using a mixture of PAC and cassava splinters binders (CSB) as the AC core and a shell with a high mechanical strength from commercial coal fly ash (CFA) and clay (CL), (ii) evaluate the SMX removal performance of the CSAC samples, and (iii) discuss the sorption characteristics and mechanism for SMX removal. Finally, this study is

Table 1
Chemical composition (wt. %) of the precursor materials used for preparing the porous ceramic shell.

Components	Coal fly ash[a] (wt. %)	Clay[b] (wt. %)
SiO_2	15.60	61.50
TiO_2	0.39	0.19
Al_2O_3	7.19	25.80
Fe_2O_3	2.96	2.84
MnO	0.06	0.03
MgO	8.25	3.45
CaO	33.52	5.23
Na_2O	0.15	0.25
K_2O	0.75	1.34
P_2O_5	0.74	0.02

[a] Coal fly ash.
[b] Clay.

expected to provide insight into potential application of a new core-shell-structure AC material with a high-mechanical-strength porous shell for the adsorption of target substances from aqueous media.

2. Experimental section

2.1. Materials and chemicals

The clay (CL) utilized in this study was collected from Rugende Valley (Kigali, Rwanda). Then, it was pre-treated at 400 °C to prevent the ceramic shell from cracking during the drying and sintering processes and sieved through a 100-mesh after cooling. The CFA and commercial PAC were provided by a coal power plant and a physical activated carbon company, respectively. The cassava waste splinters (CWS) used for preparing the CSB (Supplementary information text S1) was collected from Kinazi Cassava Plant, Rwanda. Table 1 and Table 2 present the chemical compounds contained in the CFA and CL, and the elemental composition of the CWS, PAC, and AC core, respectively. The sulfamethoxazole (SMX, purity 98%) and sulfamethazine (SMZ, purity 98%) and tetracycline (TC, purity 98%) were purchased from Alladin Industrial Corporation, Shanghai, China. The structural and physico-chemical properties of SMX are presented in Table 3. The real wastewater was withdrawn from Pig Farm of Xinluo District in Longyan, Fujian province, China.

2.2. Preparation of CSAC

The pelletizing method was used in this study [34]. Firstly, the AC core was prepared by mixing PAC with the CSB with proportions of 92% and 8%, respectively. Then, sample was pelletized to a diameter of 0.71 cm and dried at 105 °C for 2 h, which was denoted as AC core1. Secondly, the CL was mixed with CFA at the settled ratios after adding some ionized water making a mud-like mixture. The different masses of this mixture were used to coat the prepared AC core1 as a shell/cover and generate core-shell pellets These core-shell pellets were then preheated at 400 °C for 30 min after being dried at 105 °C for 2 h, and heated at 1200–1250 °C for 2 h under a nitrogen flow at a sintering rate of 10 °C min^{-1}. The CSAC materials were finally obtained after they
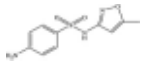
Table 2
Chemical element compositions of the cassava splinters binder, cassava splinters waste, powder activated carbon, activated carbon core used in this study.

Elements	C	N	H	O	S
CSW[a]	42.70	0.16	6.70	49.20	1.10
PAC[b]	80.42	0.10	3.84	6.20	0.35
AC core	82.62	0.43	1.26	15.26	0.20

[a] Cassava splinters waste.
[b] Powder activated carbon.

Table 3
Structure and physicochemical properties of sulfamethoxazole.

Compound name	Sulfamethoxazole
Structure [b,c,]	
Formula	$C_{10}H_{11}N_3O_3S$
Molecular weight (g mol^{-1}) [a, b]	253.28
Water solubility (mg L^{-1}) [d]	869.5
Melting point (°C) [d]	170-173
Boiling point (°C) [d]	482
pKa [a, b]	5.6
logKow [a, b]	0.89

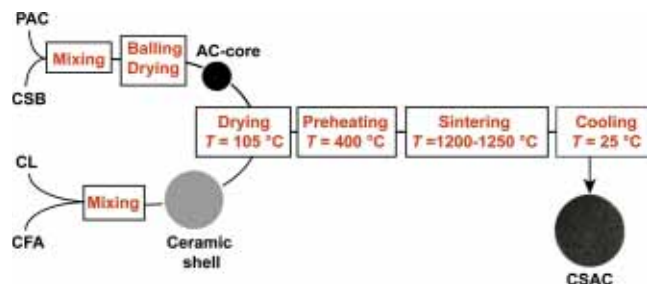[a] [14],[c] [31], [b] [32],[d] [33].

Fig. 1. Typical procedure for preparing the core-shell-structure activated carbon.

were cooled in the furnace to the ambient temperature (Fig. 1). The effects of the CFA content (10, 20, 30, and 40%), sintering temperature (1200, 1230, and 1250 °C), and shell thickness (0.08, 0.11, and 0.13 cm) on the shell's compressive strength were investigated (Fig. 2). The CSAC sample with the highest shell compressive strength was selected for characterization and used for further SMX removal.

2.3. Characterization

The crystalline, morphological features, and pore texture of the samples were characterized by powder X-ray diffraction (XRD, PANalytical X'pert Pro, Netherlands), field emission scanning electron microscopy (SEM, Hitachi S-4800, Japan), and nitrogen adsorption-desorption isotherms (Micromeritics ASAP 2020 M + C, USA), respectively. The XRD system was operated using nickel-filtered Cu-Kα (40 kV, 40 mA) radiation and a secondary monochromatic graphite beam. Brunauer-Emmett-Teller (BET) equation was used to calculate specific surface area, and the micropore and mesopore sizes were determined following the Horvath-Kawazoe (HK) and Barret-Joyner-Halenda (BJH) methods, respectively. Adsorbent samples (5%) were mixed with spectroscopic grade KBr and finely ground in a mortar. The samples were measured against a KBr background. 32 scans at a resolution of 4 were collected. A ZL-8001 computer servo universal material testing machine (China) was used to measure the mechanical strength of the CSAC, and the zeta potential of the CSAC was tested using a Nano/submicron particle size analyzer (Zeta PALS). Further analyses were conducted for C, H, N, O, and S in a Thermo Flash 1112 analyzer. The chemical composition of the CFA and clay were tested by X-ray fluorescence spectroscopy using a Philips PW1404 device.

2.4. Adsorption of SMX

Batch experiments were carried out by adding 0.5 g of CSAC to 50 mL of the SMX solution in an Erlenmeyer flask at 25 °C in a water bath and oscillating at a rate of 150 r min^{-1} for 24 h. The supernatant
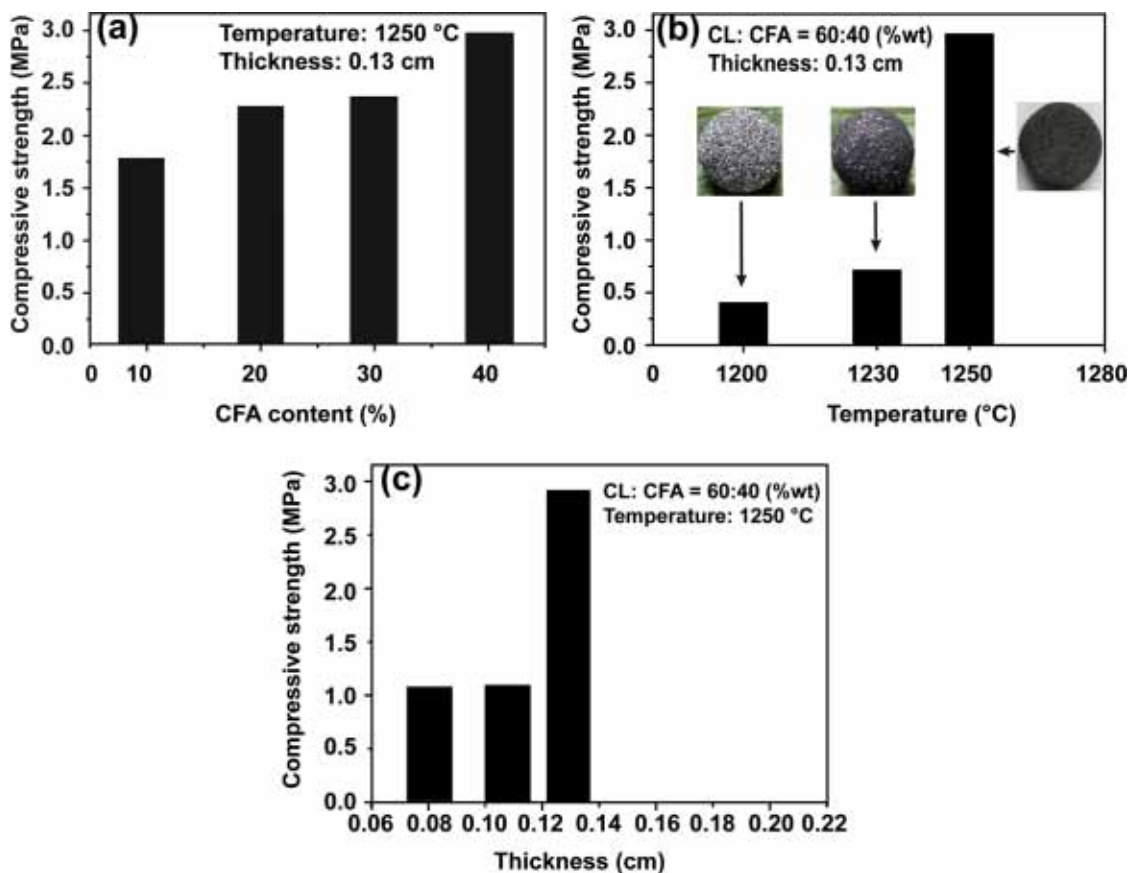

Fig. 2. Optimization of core-shell-structure activated carbon preparation.

samples were withdrawn and then filtered through a 0.45-μm membrane. The water samples were analyzed using high-performance liquid chromatography (HPLC, Hitachi L-2000, Japan) at 25 °C with a wavelength of 225 nm, using an Extend-C18 column (250 × 4.6 mm, 5-Micron 80 A) from Agilent (USA). The antibiotics in the real wastewater were analyzed by LC–MS. More details have been presented in Supplementary information text S2.

Initial SMX concentrations of 5, 10, 30, 50 and 100 mg L^{-1} in the SMX solution were prepared by diluting the bulk SMX solution, and the tests were conducted at an initial pH of 5.6. Solutions with different pH values (1.0, 2.0, 4.0, 5.6, 7.0, 9.0 and 12.0) were produced by adjusting the initial solution using 0.01 mol L^{-1} of NaOH or HCl. The effect of these pH values was tested at an initial SMX concentration of 100 mg L^{-1} at 25 °C. Supernatant samples were collected at specific time within 480 min at pH of 5.6, temperature of 25 °C and 50 mg L^{-1} SMX solutions. To test the regeneration performance of the adsorbents, the CSAC after absorbing SMX was recycled by thermal treatment at 600 °C for 1 h under a N$_2$ atmosphere. This temperature was preferred because SMX degrades when the temperature is below 600 °C [35]. The regenerated material was reutilized for further adsorption experiments. Three kinetics models, i.e., the pseudo-first-order and second-order models, and intraparticle diffusion, were used to fit the adsorption kinetics data of SMX by CSAC. In addition, experimentally acquired adsorption isotherms were explained using Langmuir and Freundlich models [8,14,36]. The kinetic and isotherm models are described in Supplementary information text S3. The antibiotics from real wastewater were withdrawn by solid phase extraction method according to this study [37].

3. Results and discussion

3.1. Optimized synthesis of CSAC

The synthesis conditions were optimized to obtain a CSAC material with a relatively high compressive strength by manipulating mixture ratio of CL and CFA, the sintering temperature, and the shell thickness. Fig. 2a showed that the compressive strength of the shell was approximately 2.92 MPa at a CFA ratio of 40 wt. %. The high compressive strength was beneficial from the formation of the quartz phase, mullite, and glass phases at 1250 °C, which was proven by several studies [38,39]. A CFA content of 40% with a compressive strength of 2.92 MPa was considered to be favorable to create a material that can withstand the decrease in pressure in the absorption column. Fig. 2b illustrated that the shell's compressive strength increased as the sintering temperature increased, at a constant CL and CFA ratio of 60 and 40 (wt. %). The compressive strength was approximately 0.4 MPa when the temperature was 1200 °C, while it increased greatly to 2.92 MPa at a sintering temperature of 1250 °C. This was attributed to the formation of mullite, quartz, crystalline, and the glassy phase at 1250 °C. Fig. 2c presented that the shell's compressive strength increased as its thickness increased. For instance, the compressive strength was approximately 1.0 MPa when the thickness was 0.11 cm, while it greatly increased to 2.92 MPa when the thickness was 0.13 cm. Therefore, the optimal conditions for the synthesis of CSAC was a CL:CFA ratio of 60:40 (wt. %), sintering temperature of 1250 °C, and shell thickness of 0.13 cm. The product generated under these conditions was used for SMX absorption.

3.2. Characterization

The morphological properties of the samples were observed by SEM at different magnifications (Fig. 3). As shown in Fig. 3a and b, there were many fine pores and macropores in the optimized ceramic shell. Moreover, Fig. 3c and d show that capillary-like pore structures were developed on the AC core's surface, and some particulate matters appeared on the external surface of the AC core. These pores were

originated from the evaporation or decomposition of matter in the binder or chemical reactions between the AC and the binder [40,41]. The images of the CSAC and the AC core (inside the shell) can be visually examined by the naked eye in Fig. 3e and f. The pore sizes of the prepared samples varied notably due to the preparation temperature. The results indicated that the prepared material possessed a rich pore structure.

Fig. 4 presents the representative XRD patterns of the porous ceramic shell, clay, and CFA. The XRD patterns of CFA in Fig. 4a indicated the presence of calcium magnesium carbonate (CaMg(CO$_3$)$_2$), calcium carbonate (CaCO$_3$), and quartz (SiO$_2$). Fig. 4b exhibits the presence of quartz (SiO$_2$) and aluminum silicate hydrate in the clay. The XRD patterns of the shell for CSAC (Fig. 4c) indicated the existence of anorthic, quartz (SiO$_2$), calcium, magnesium, aluminum silicates, and mullite species. Based on these findings, the crystalline quartz, anorthite, and sapphirine were trailing phases as long as the preparation temperature was below 1200 °C. Alkaline, calcium, and iron-containing crystalline phases would melt and then form a glassy phase at temperatures exceeding 1200 °C, therefore, they were not detected in the CSAC XRD patterns [42].

The textural pore parameters, including the specific surface area (S$_{BET}$), pore volume, and pore size, are listed in Table 4. It is noteworthy that AC core2 was directly separated from the CSAC, and it exhibited a higher S$_{BET}$ (1095 m^2 g^{-1}). The S$_{BET}$ of PAC decreased from 823 to 664 m^2 g^{-1} after mixing with CSB (AC core1). This decline was due to the blocking of free space and pores as previously reported [43,44]. The PAC used for preparing AC core1 has a smaller S$_{BET}$ (823 m^2 g^{-1}) than that of the AC core2 (1095 m^2 g^{-1}), which is because the higher temperature caused an increase in the S$_{BET}$ for both binders and binder-bonded carbon pellets [45]. The S$_{BET}$ of CSAC (181 m^2 g^{-1}) was much smaller than that of AC core2 without the shell, which is due to two reasons. One was associated with the blocking of pores in AC core2 by the piles (agglomerates) of the ceramic shell, and the other was that the shell weight was included in the denominator. The surface area of the CL-CFA mixture (raw materials of the shell) was 30 m^2 g^{-1}. However, it decreased to 2.9 m^2 g^{-1} after sintering as CSAC. Furthermore, the pore volume of AC core1 shrunk to a greater degree than that of the PAC. In contrast, the pore volume of AC core2 was larger than that of the PAC. However, the pore volume of CSAC decreased due to the protection of AC core2 by the porous ceramic shell and sintering at a high temperature. The pore volume of the shell detached from CSAC also significantly decreased after sintering the raw CL-CFA mixture at 1250 °C. The pore sizes of PAC, AC core1, AC core2, and CSAC did not change significantly, while that of the CL-CFA mixture decreased after the CSAC was heated at 1250 °C. Fig. 5 shows that the pore size distribution curves shifted toward a large pore size for all materials. AC core1 and PAC exhibited similar pore size distributions, suggesting the coexistence of micropores and mesopores due to intra-particle voids (Fig. 5a). The pore size distribution of CSAC and AC core2 was noticeably broadened and shifted to large pore sizes due to the sintering of the sample at 1250 °C (Figs. 5a and 5b). In addition, the pore size distribution of CL-CFA and the shell of CSAC exhibited a broad pore size with micro-mesopores and macropores (Fig. 5c and d). However, the macropore distribution increased after sintering at 1250 °C (Fig. 5d), which is beneficial for the molecular diffusion of SMX from the shell into the AC core.

3.3. Application to SMX removal

3.3.1. Effect of initial SMX concentration

As shown in Fig. 6a, 99.0% and 97.9% of SMX were removed by the CSAC adsorbent at initial concentrations of 5 and 10 mg L^{-1}, respectively. Moreover, SMX was partly removed with 77.0, 68.8, and 60.4% efficiencies at initial concentrations of 30, 50, and 100 mg L^{-1}, respectively. Additionally, similar results were obtained for PAC and AC core2 when initial SMX concentrations were 5 and 10 mg L^{-1}.
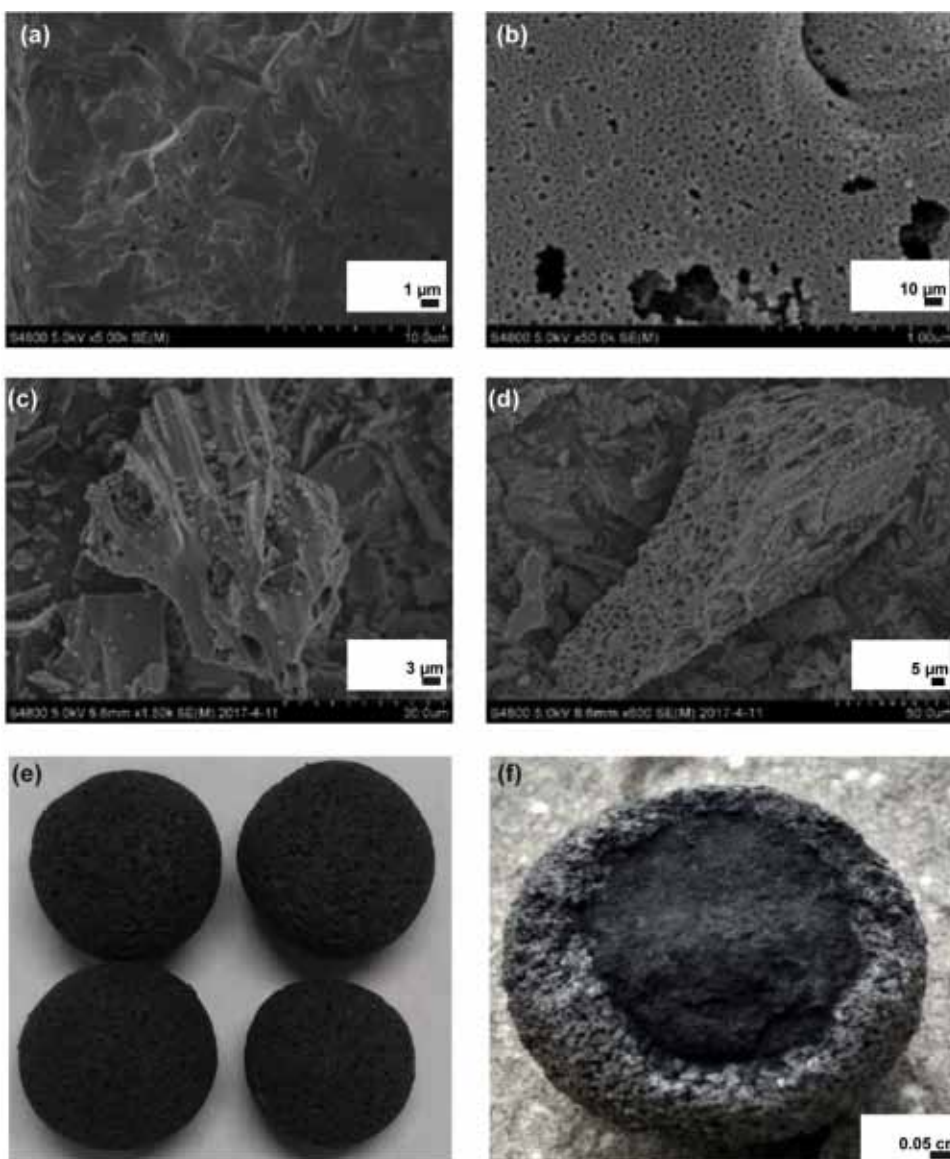
Fig. 3. SEM images of the ceramic shell's surface (a, b) and activated carbon core2 (c, d), images of Core-shell-structure activated carbon (e) and the inside of the activated carbon core2 shell (f).
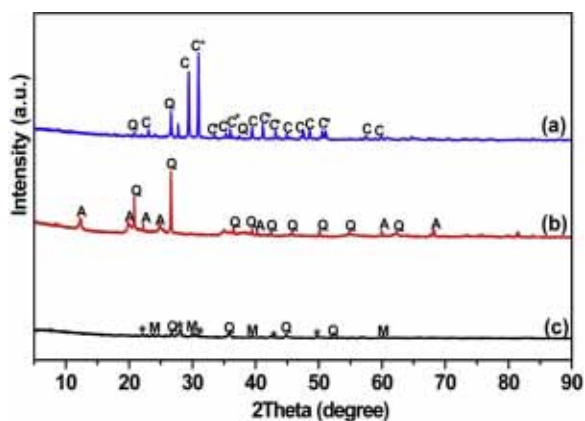

Fig. 4. XRD patterns for coal fly ash (a), clay (b), and the ceramic shell (c) (A: Aluminum silicate hydrate, Q: Quartz, C: Calcium carbonate, C*: Calcium magnesium carbonate, *: Anorthic, M: Calcium magnesium aluminum silicate, and M*: Mullite).

Table 4
Specific surface area (S_{BET}), pore volume, and pore size of the materials used in this study.

Sample	Thickness (cm)	Weight (g)	S_{BET} ($m^2 g^{-1}$)	Pore volume ($\times 10^{-2}$ cm^3 g^{-1})	Pore size (nm)
CSAC	0.13	0.50	181	10.12	2.238
Shell	–	0.20	2.9	0.24	3.134
PAC	–	0.05	823	44.17	2.147
AC core1*	–	0.10	664	34.99	2.109
AC core2*	–	0.05	1095	59.24	2.164
CL-CFA	–	0.30	30	8.66	12.000

AC core1*: AC core after drying at 105 °C; AC core2*: AC core from CSAC.

Meanwhile, for the SMX solutions with other concentrations, AC core2 removed 97.0, 95.4, and 95.1%, and PAC removed 90.0, 78.0, and 76.0% of SMX, respectively. These results could be explained by the constant reactive sites under the same amount of adsorbent [46]. The adsorption capacity increases as the initial concentration of the adsorbate increases, suggesting that the initial concentration is a key factor in overcoming the mass transfer between the adsorbate and AC
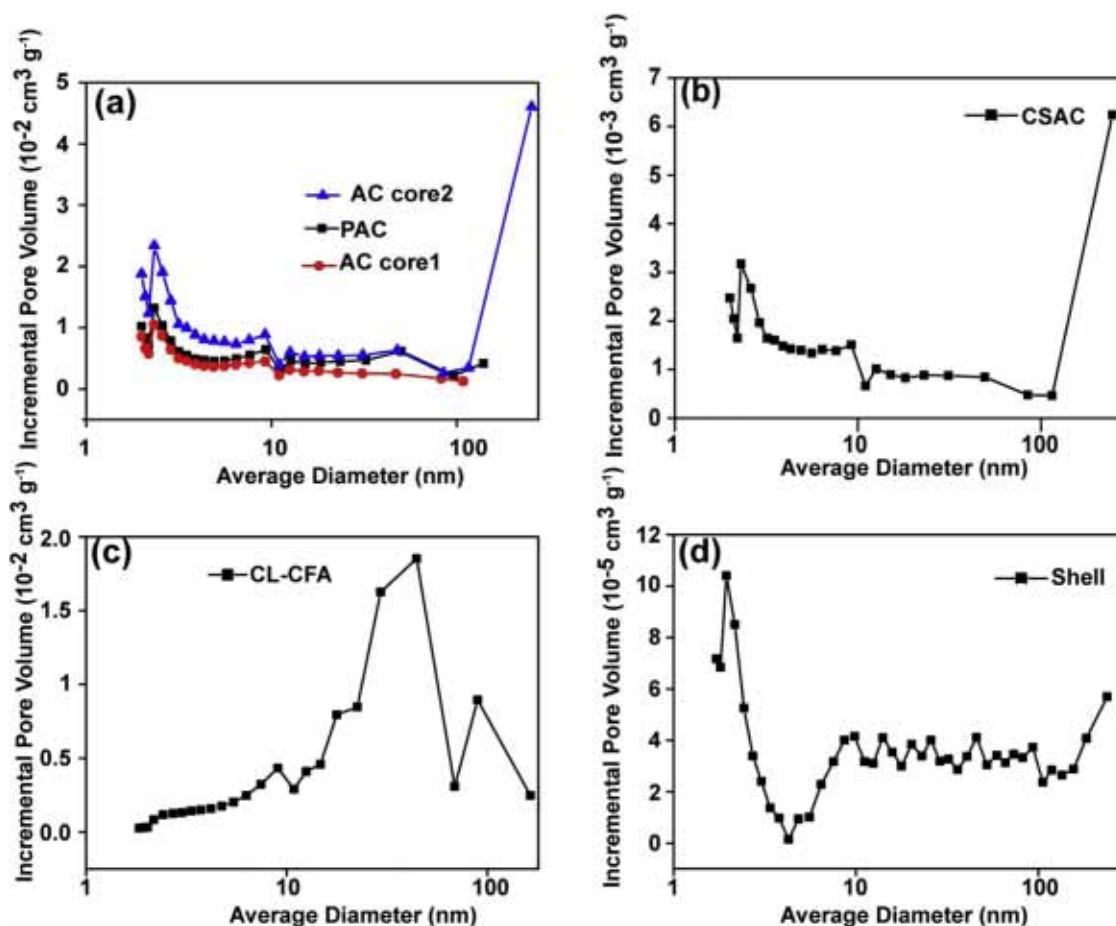
Fig. 5. Pore size distribution for the powder activated carbon, activated carbon-core1, and activated carbon-core2 (a); Core-shell-structure activated carbon (b); raw materials of the clay-coal fly ash shell (c) and of the CSAC shell after sintering at 1250 °C (d).

[47]. From the experimental observations, it was found that the adsorption of CSAC decreased comparatively to AC core2 and PAC, however, the CSAC still showed easy separation, recyclability and good performance over recycling life cycle.

3.3.2. Effect of initial pH

The SMX removal by CSAC was highly affected by the initial pH of the solution. The pH not only affected surface properties of CSAC, but also determined species of SMX in the solution. Fig. 6b shows that the solution's pH was responsible for the SMX removal efficiency. An acidic pH enhances the SMX removal efficiency and capacity. In contrast, the values decreased as the pH increased from 4.0 to 12.0. Fig. 6d shows that pH_{PZC} (the pH at the point of zero charge) was 1.88, indicating that the surface of the CSAC had negative charges when the pH value exceeded the pH_{PZC}. Cationic (SMX^+), neutral (SMX), and anionic (SMX^-) compounds were formed based on two acid dissociation constants within a wide pH range. The first constant involves the protonation of the aniline N (pKa = 1.7) and the other entails deprotonation of the sulfa drug's NH (pKa = 5.6) [48]. When the pH increased from 1.0 to 12.0, the SMX^+ gradually transformed into SMX, and then SMX^-. At pH 5.6, the concentrations of SMX and SMX^- were equal. Therefore, when the pH equaled to 1.88, the dominant compound was SMX^+ and the surface charge of CSAC was negative, thus, the electrostatic attraction favored the adsorption of SMX. Additionally, after pH increase to or more than 5.6, the adsorption efficiency of SMX decreased due to the decreasing of electrostatic attraction between the adsorbent and SMX. This correlates with the findings of previous reports [31,48–51].

3.3.3. Effect of contact time

As illustrated in Fig. 6c, the removal reached the equilibrium within 360 min of adsorption. The SMX removal efficiency by CSAC increased with increasing contact time. This is because the solution firstly crossed the ceramic shell and continuously diffused into the AC core until it reached the equilibrium within approximately 360 min. Similarly, the SMX removal efficiency by AC core2 separated from CSAC sharply increased at 120 min, and then slowly increased until reaching the equilibrium at approximately 360 min, which was the same time as that of CSAC. However, the removal efficiency of AC core2 was greater than that of CSAC due to the protection from the ceramic shell, which served as an obstacle to transfer of SMX solution from the bulk solution to the AC core's surface. In contrast, the SMX removal efficiency of PAC was much faster than that of CSAC and AC core2, and was initially rapid and reached the equilibrium at approximately 60 min. This was a result of the large number of available reactive sites on PAC and the rapid mass transport of SMX solution through the PAC. Furthermore, the q_t of SMX adsorption by the AC core inside the ceramic shell was calculated using the mass of the AC core inside the shell as the denominator, and the results show that the q_t was slightly less than that of PAC and AC core2 (Fig. 6e). This indicates that the ceramic shell slightly affected the SMX adsorption capacity and efficiency. More importantly, the CSAC still showed easy separation, recyclability and good performance over recycling life cycle.

3.3.4. Thermal regeneration of CSAC

The recycling and regeneration of CSAC material are critical factors for its practical application. The used samples were regenerated and used for SMX adsorption for a further three cycles. As shown in Fig. 7,
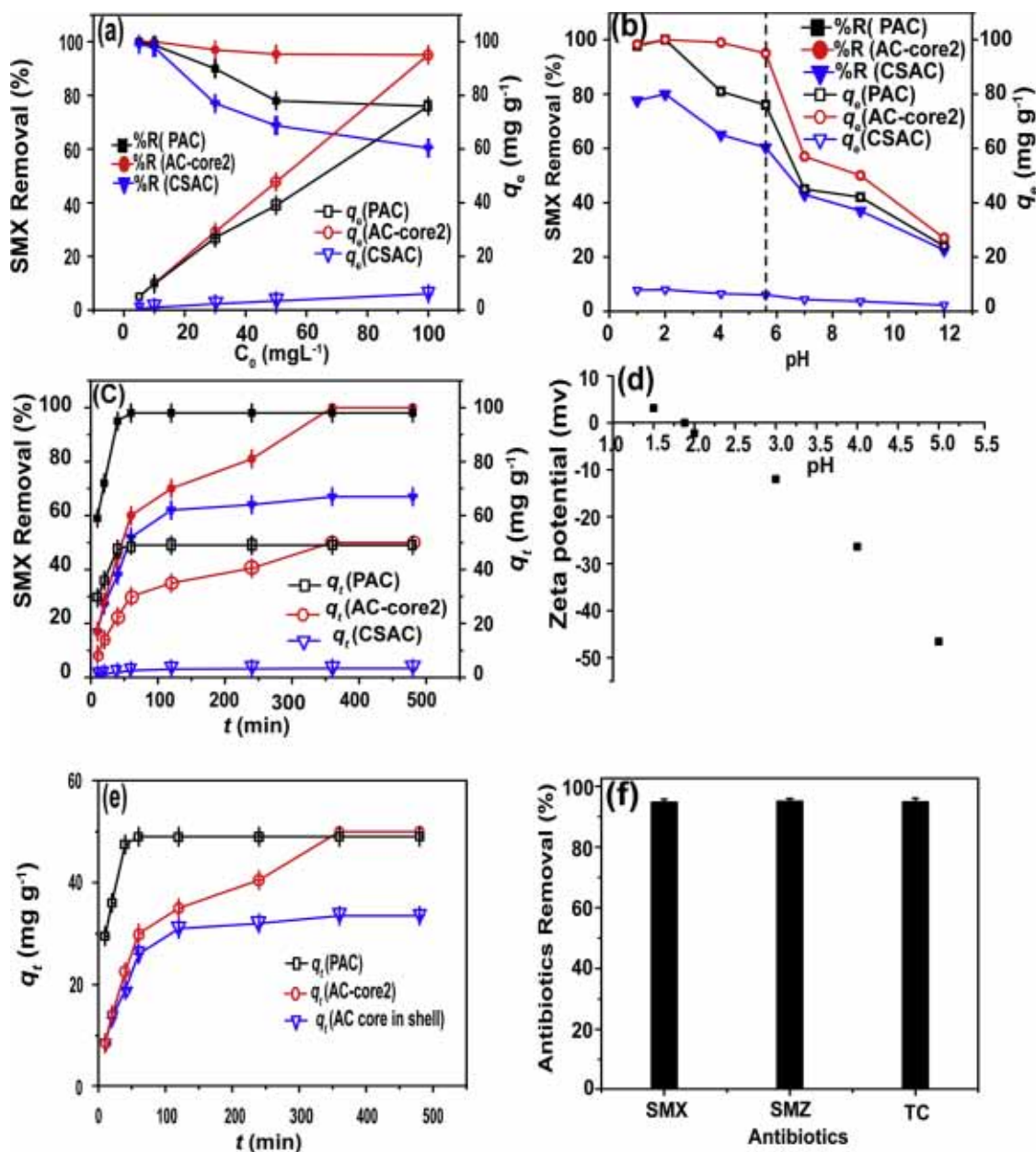
Fig. 6. Effects of initial concentration (a), pH (b), contact time ((c) and (e)) on the adsorption of SMX, the pH$_{PZC}$ of core-shell-structure activated carbon (d), and adsorption of antibiotics in real wastewater (f).
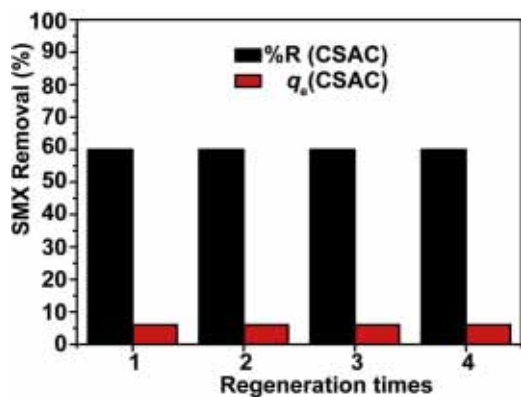

Fig. 7. Adsorption of sulfamethoxazole on core-shell-structure activated carbon at an initial concentration of $100\,mg\,L^{-1}$ after thermal regeneration.

the generated CSAC exhibited a comparable adsorption capability to that of the original CSAC.

3.4. Sorption kinetics and isotherm

3.4.1. Sorption kinetics

Table 5 presents the parameters of the calculated kinetics based on the experimental results. The parameters such as the correlation coefficients (R^2), kinetics constants (k_1), and q$_e$ values were estimated by plotting $\ln(q_e - q_t)$ against t (pseudo-first-order model) and t/qt against t (pseudo-second-order model). SMX adsorption fitted better to the pseudo-second-order kinetic model according to the calculated correlation coefficient ($R^2 \geq 0.996$) and small difference between q_e^{exp} and q_e^{cal}. This result was consistent with that in previous report on organic matter removal by activated carbon [14,49]. Additionally, intraparticle diffusion was a rate-determining stage in the adsorption process. According to the R^2 values ($R^2 \leq 0.898$), the sorption process was not

Table 5

Kinetic parameters of sulfamethoxazole adsorption.[a]

Kinetic model	Parameters		
	CSAC	AC core2	PAC
q_e [exp] (mg g^{-1})	3.4	47.7	39.0
Pseudo-first-order			
q_e calculated (mg g^{-1})	2.06	34.7	37.4
K_1	7.48×10^{-3}	7.02×10^{-3}	0.102
R^2	0.724	0.907	0.846
Pseudo-second-order			
q_e [cal] (mg g^{-1})	3.7	53.0	39.3
K_2	7.53×10^{-3}	0.336×10^{-3}	11.75×10^{-3}
R^2	0.997	0.996	0.999
Intraparticle-diffusion			
C	0.98	8.10	32.00
K_{dif}	0.13	2.03	0.39
R^2	0.798	0.898	0.355

[a] Adsorption conditions: initial concentration = 50 mg L^{-1}, mass of adsorbents = 0.5 and 0.05 g, agitation speed = 150 *rpm*, temperature = 25 °C, and pH = 5.6.

determined by intraparticle diffusion. A multi-linear plot by q_t against $t^{1/2}$ indicated the presence of multiple steps in the adsorption process, which correlates with previously reported findings [52]. The SMX adsorption process could consist of three steps: rapid external surface sorption, involving the mass transfer of SMX to the external adsorbent surface; gradual interior surface sorption, which involves the mass transfer of SMX onto the internal surface; and the last step, in which the equilibrium reaches and the adsorption efficiency declines.

3.4.2. Sorption isotherm

The data calculated from the Langmuir and Freundlich models is presented in Table 6. The R^2 values demonstrate that the Freundlich isotherm fitted more precisely than the Langmuir isotherm, revealing that SMX adsorption was consistent with multilayer adsorption. The n of Freundlich model is associated with the SMX sorption affinity on the adsorbent. Generally, n at the ranges of 2–10, 1–2 and less than 1 represent good adsorption, moderate adsorption and poor adsorption, respectively. The n value (2.65) in Table 6 indicated a good adsorption of SMX on CSAC. The parameter K$_F$ of Freundlich model is related to the sorption amounts for the adsorbents. The value for CSAS as the adsorbent is smaller than those of AC and PAC, indicating the low sorption amounts of SMX on the CSAC. However, as shown in Fig. 6e, results show that the q$_t$ was slightly less than that of PAC and AC core2. Based on the Langmuir model, the adsorption capacity of the adsorbents was determined and the results demonstrated that the adsorption capacity of the AC core2 was greater than that of PAC and CSAC. This was likely due to the larger S$_{BET}$ of AC core2 and the mass transfer obstacle in the AC core2 protected by the ceramic shell. The adsorption capacity (q$_e$) of

Table 6

Adsorption isotherm parameters of sulfamethoxazole adsorption.[a]

Adsorption isotherm model	Parameters		
	CSAC	PAC	AC core2
Langmuir isotherm			
q_m (mg g^{-1})	6.4	86.0	95.4
k_L (L mg^{-1})	0.15	8.41×10^{-4}	1.00×10^{-4}
R^2	0.826	0.770	0.643
Freundlich isotherm			
k_F (mg g^{-1}) (L mg^{-1}) 1/n	1.3	14.2	28.0
n	2.65	2.12	1.34
R^2	0.945	0.933	0.978

[a] Adsorption conditions: initial concentration = 5, 10, 50, 80, and 100 mg L^{-1}, mass of adsorbents = 0.5 and 0.05 g, agitation speed = 150 *rpm*, temperature = 25 °C, and pH = 5.6.

Table 7

. Comparison of sulfamethoxazole adsorption capacity on Core-shell-structure activated carbon with other adsorbents.

Pollutant	Adsorbents	q_m (mg g^{-1})	References
SMX	CSAC	6.3	This work
	AC core2	95.4	This work
	PAC	86	This work
	PAC-II[a]	58.35	[14]
	CNT[b]	28.88	[14]
	GNS[c]	103	[49]
	GOS[d]	122	[49]

[a] commercial powdered activated carbon from coal.
[b] carbon nanotube.
[c] graphene nanosheet.
[d] graphene oxide nanosheet.

the adsorbents used in this work was relatively beneficial, as mentioned in (Table 7), compared with other adsorbents [14,49].

3.5. Possible mechanism

Electrostatic and non-electrostatic interactions are phenomena implied in the adsorption process [46]. The adsorption of aromatic species on AC is highly affected by the diffusive interaction between the π-electrons of the aromatic ring and the π-electrons of the graphene layers in AC [51,53]. However, the mechanisms governing the adsorption of sulphonamide to carbon adsorbents are still unclear [15]. Fig. 8 presents conceptually the mechanism behind the removal of SMX by CSAC. As shown in the inserted FTIR figure in Fig. 8, adsorption of SMX resulted in the appearance of new bands at 1590, 1473, 1380, 1145, 1090, 884 and 829 cm^{-1}. They are corresponding to phenyl ring C = C, isoxazole ring, SO$_2$, SN and isoxazole ring CH, respectively [23]. This outcome indicated that the SMX molecular was adsorbed on the surface of the AC core. The adsorption of SMX by CSAC simultaneously depends on the pore texture, π-π electro-donor acceptor (EDA), electrostatic interactions, and the hydrophobic properties of the SMX molecule, which are determined by the surface charge of the CSAC and acid dissociation of the SMX that are dependent on variations in the solution's pH.

3.5.1. (a) Pore texture

A previous study found that more SMX is adsorbed on adsorbents with pores volume larger than 20 Å, suggesting that mesopores are beneficial for the adsorption of SMX [23]. As shown in Fig. 5, all adsorbents have pore volumes larger than 20 Å, suggesting that CSAC and the other adsorbents could adsorb more SMX from an aqueous solution. The pathways of SMX adsorption to CSAC can be described as follows: SMX molecules easily pass through the shell due to its macropores and results confirmed by FTIR analysis, the SMX molecules then reach the external surface of AC core2, and they are finally diffused into the inner surface pores of AC core2.

3.5.2. (b) electrostatic, π-π interactions and hydrophobicity

The SMX as a sulfonamides group, may undergo pH-dependent speciation reactions [12,15,48]. Based on the two dissociation SMX constants (pKa = 1.7 and pKa = 5.6) throughout a broad pH range, there are three dominant forms, i.e., anionic (SMX$^-$), neutral (SMX), and cationic (SMX$^+$) [48]. The first acid dissociation constant (pKa = 1.7) involves the protonation of aniline N, and the second (pKa = 5.6) involves deprotonation of the sulphonamide NH. At pH levels exceeding 5.6, SMX$^-$ is predominant, while uncharged SMX is predominant at pH values between 1.7 and 5.6, and SMX$^+$ predominates at pH values below 1.7 [54]. The pH$_{PZC}$ value of CSAC was 1.88 (Fig. 6d). At a lower pH value (1.0), electrostatic repulsion is established between the cationic SMX and positively charged CSAC, which decreases the SMX
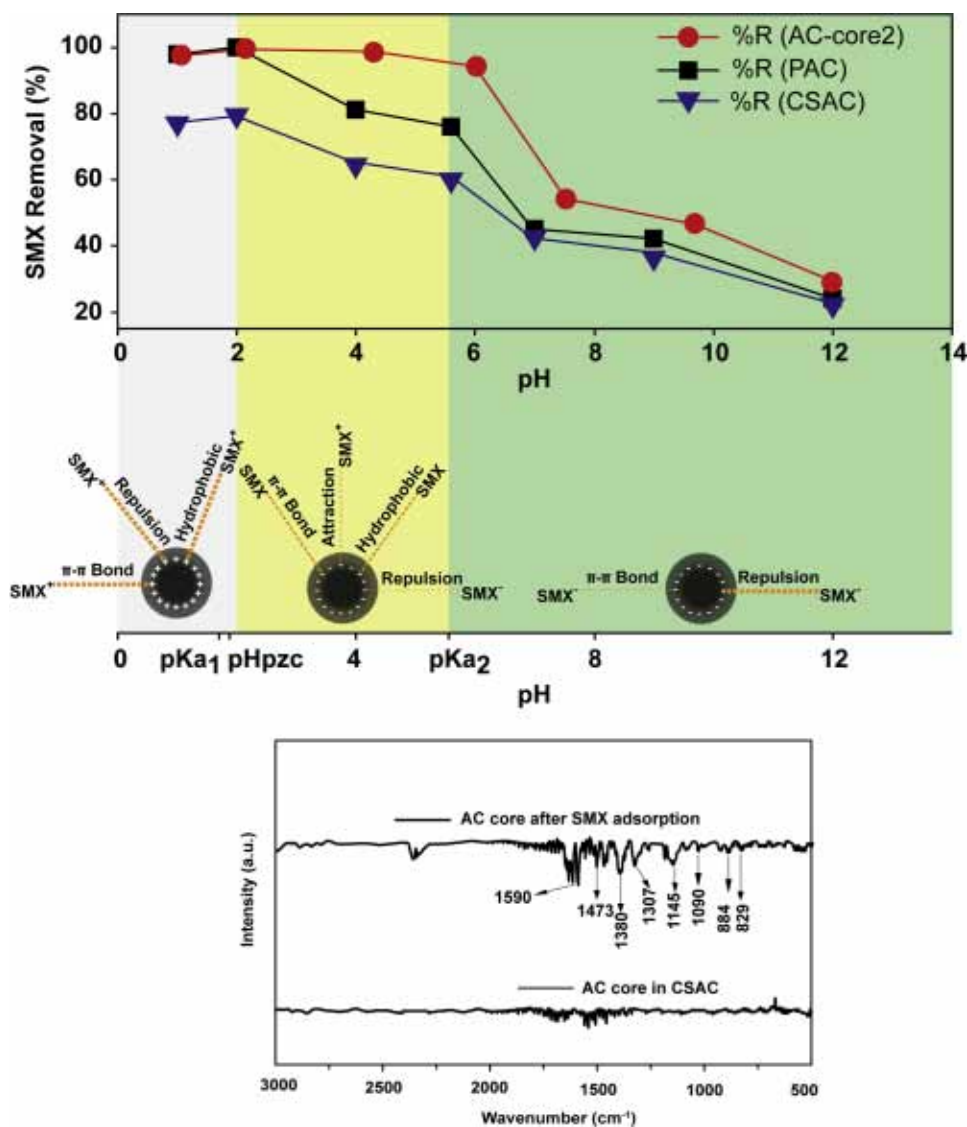
Fig. 8. Mechanism for the adsorption of sulfamethoxazole on core-shell-structure activated carbon.

adsorption efficiency of CSAC. It is noteworthy that SMX was partly transformed from its neutral form into negative species within pH values ranging from 5.6 to 7.0, which leads to the electrostatic repulsion among the anionic surfaces of CSAC and SMX$^-$. Additionally, within pH values ranging from 7.0 to 12.0, the presence of neutral SMX species decreased and anionic species became dominant. The electrostatic repulsion between the anionic CSAC surface and the SMX$^-$ was unfavorable for the uptake of SMX.

Moreover, SMX is a strong π-acceptor due to its functional amino groups and N-hetero aromatic rings [12]. The noncovalent attractive π-π EDA force taking place between π-donors (electro–rich arenes) and π-acceptors (electro-poor arenes) is also described as a mechanism depicting the strong interactions between black carbon and nitroaromatics [55,56]. The ability of the π-acceptor for SMX$^+$ increased and thus π-π EDA interactions increased. Therefore, the efficiency of the SMX adsorption on CSAC was regulated by different interactions and pH value below 2 (approximately 1.88), where the π-π EDA, hydrophobic properties and weak electrostatic attraction simultaneously favored the adsorption of SMX. Furthermore, another SMX adsorption mechanism on CSAC was hydrophobic interactions. According to previous studies [57,58], the hydrophobic properties of SMX are pH-dependent. For example, at pH values below the second dissociation constant (pKa = 5.6), hydrophobic partitioning with organic compound

dominates because of the nonionic nature of SMX, which is beneficial for SMX adsorption. In addition, higher pH values result in weak π-π EDA interactions between SMX and CSAC. This phenomenon is consistent with the findings of previous studies [15,59–61].

3.6. Adsorption study of SMX in real waste water

The three antibiotics, including SMX, SMZ and TC, were detected in real wastewater. Their concentrations were 1860, 831 and 892 ug/L, respectively. Different antibiotics at concentration of 200 ug/L were spiked into the real wastewater. The recovery was calculated based on the concentration of antibiotics in real wastewater and spiked wastewater. The recovery of SMX, SMZ and TC were 99.25, 99.60 and 99.00%, respectively. As shown in Fig. 6(f), the simultaneous adsorption efficiency of SMX, SMZ and TC by CSAC were 94.68, 95.02, and 94.80%, respectively. These results proved that the CSAC sample exhibited a good performance for antibiotics removal from a real wastewater.

4. Conclusions

In this study, a novel core-shell-structure activated carbon (CSAC) material was successfully synthesized and utilized to remove

sulfamethoxazole (SMX) from water. The results showed that the shell had a high compressive strength of 2.92 MPa when its thickness was 0.13 cm, the clay (CL) and coal fly ash (CFA) mixture ratio was 60 and 40 (wt. %), and the sintering temperature was 1250 ˚C. The AC core was synthesized using commercial powder AC (92%) mixed with a binder (8%) created from cassava waste splinters (CWS). The CSAC exhibited two roles resulting from the AC core and porous ceramic shell, which synergistically adsorbed SMX from aqueous solutions. In addition, the CSAC material exhibited a good performance of antibiotics removal from real wastewater. The adsorption isotherm showed that the Freundlich isotherm fitted better than the Langmuir isotherm. The CSAC was also found to be recyclable and could be regenerated at 600 ˚C. The possible mechanism for SMX adsorption indicated that the adsorption of SMX on CSAC simultaneously depends on pore texture, π-π EDA, electrostatic interactions, and hydrophobic properties of SMX molecules, which are determined by the surface charges of CSAC and the acid dissociation constants of SMX that are dependent on variations in solution pH.

Acknowledgements

Appendix A. Supplementary data

Supplementary material related to this article can be found, in the online version, at doi:https://doi.org/10.1016/j.jhazmat.2019.01.093.

References

[1] I.-S. Lee, S.-H. Lee, J.-E. Oh, Occurrence and fate of synthetic musk compounds in water environment, Water Res.. 44 (2010) 214–222.

[2] J.-L. Liu, M.H. Wong, Pharmaceuticals and personal care products (PPCPs): A review on environmental contamination in China, Environ. Int. 59 (2013) 208–224.

[3] C.I. Kosma, D.A. Lambropoulou, T.A. Albanis, Investigation of PPCPs in wastewater treatment plants in Greece: occurrence, removal and environmental risk assessment, Sci. Total. Environ. 466 (2014) 421–438.

[4] D.Q. Zhang, R.M. Gersberg, W.J. Ng, S.K. Tan, Removal of pharmaceuticals and personal care products in aquatic plant-based systems: A review, Environ. Pollut. 184 (2014) 620–639.

[5] E.N. Evgenidou, I.K. Konstantinou, D.A. Lambropoulou, Occurrence and removal of transformation products of PPCPs and illicit drugs in wastewaters: a review, Sci. Total. Environ. 505 (2015) 905–926.

[6] P. Schroder, B. Helmreich, B. Skrbic, M. Carballa, M. Papa, C. Pastore, Z. Emre, A. Oehmen, A. Langenhoff, M. Molinos, J. Dvarioniene, C. Huber, K. Tsagarakis, E. Martinez-Lopez, S. Pagano, C. Vogelsang, G. Mascolo, Status of hormones and painkillers in wastewater effluents across several European states-considerations for the EU watch list concerning estradiols and diclofenac, Environ. Sci. Pollut. R. 23 (2016) 12835–12866.

[7] A.J. Ebele, M. Abou-Elwafa Abdallah, S. Harrad, Pharmaceuticals and personal care products (PPCPs) in the freshwater aquatic environment, Emerg. Contam. 3 (2017) 1–16.

[8] J. Akhtar, N.S. Amin, A. Aris, Combined adsorption and catalytic ozonation for removal of sulfamethoxazole using Fe_2O_3/CeO_2 loaded activated carbon, Chem. Eng. J. 170 (2011) 136–144.

[9] S.E. Jorgensen, B. Halling-Sorensen, Drugs in the environment, Chemosphere 40 (2000) 691–699.

[10] X.L. Bai, K. Acharya, Removal of trimethoprim, sulfamethoxazole, and triclosan by the green alga Nannochloris sp, J. Hazard. Mater. 315 (2016) 70–75.

[11] K.M. Dimpe, A. Mpupa, P.N. Nomngongo, Microwave assisted solid phase extraction for separation preconcentration sulfamethoxazole in wastewater using tyre based activated carbon as solid phase material prior to spectrophotometric determination, Spectrochim Acta A. 188 (2018) 341–348.

[12] D. Zhang, B. Pan, H. Zhang, P. Ning, B. Xing, Contribution of different sulfamethoxazole species to their overall adsorption on functionalized carbon nanotubes, Environ. Sci. Technol. 44 (2010) 3806–3811.

[13] C.O. Ania, J.B. Parra, J.A. Menendez, J.J. Pis, Microwave-assisted regeneration of activated carbons loaded with pharmaceuticals, Water Res. 41 (2007) 3299–3306.

[14] M.C. Tonucci, L.V.A. Gurgel, S.F. de Aquino, Activated carbons from agricultural byproducts (pine tree and coconut shell), coal, and carbon nanotubes as adsorbents for removal of sulfamethoxazole from spiked aqueous solutions: kinetic and thermodynamic studies, Ind. Crop. Prod. 74 (2015) 111–121.

[15] L.L. Ji, W. Chen, S.R. Zheng, Z.Y. Xu, D.Q. Zhu, Adsorption of sulfonamide antibiotics to multiwalled carbon nanotubes, Langmuir 25 (2009) 11608–11613.

[16] D.R.S. Lima, B.E.L. Baeta, S.F. Aquino, M. Libanio, R.J.C.F. Afonso, Removal of pharmaceuticals and endocrine disruptor compounds from natural waters by clarification associated with powdered activated carbon, Water Air Soil.Poll. 225 (2014) 2170.

[17] N. Vieno, T. Tuhkanen, L. Kronberg, Removal of pharmaceuticals in drinking water treatment: effect of chemical coagulation, Environ. Technol. 27 (2006) 183–192.

[18] V. Saritha, N. Srinivas, N.V. Srikanth Vuppala, Analysis and optimization of coagulation and flocculation process, Appl. Water Sci. 7 (2017) 451–460.

[19] E.K. Putra, R. Pranowo, J. Sunarso, N. Indraswati, S. Ismadji, Performance of activated carbon and bentonite for adsorption of amoxicillin from wastewater: mechanisms, isotherms and kinetics, Water Res. 43 (2009) 2419–2430.

[20] S.A. Snyder, P. Westerhoff, Y. Yoon, D.L. Sedlak, Pharmaceuticals, personal care products, and endocrine disruptors in water: implications for the water industry, Environ. Eng. Sci. 20 (2003) 449–469.

[21] F. Yu, F. Li, S. Han, J. Ma, Adsorptive removal of antibiotics from aqueous solution using carbon materials, Chemosphere 153 (2016) 365–385.

[22] E.E. Chang, J.C. Wan, H. Kim, C.H. Liang, Y.D. Dai, P.C. Chiang, Adsorption of selected pharmaceutical compounds onto activated carbon in dilute aqueous solutions exemplified by acetaminophen, diclofenac, and sulfamethoxazole, Sci. World J.. (2015) 1–11 2015.

[23] L. Nielsen, M.J. Biggs, W. Skinner, T.J. Bandosz, The effects of activated carbon surface features on the reactive adsorption of carbamazepine and sulfamethoxazole, Carbon 80 (2014) 419–432.

[24] F. Cecen, Ö. Aktaş, Ferhan Çeçen, Özgür Aktaş, Activated Carbon for Water and Wastewater Treatment: Integration of Adsorption and Biological Treatment, Wiley-VCH, 2011, p. 388 ISBN: 978-3-527-32471-2.

[25] Z.J. Wu, L.J. Kong, H. Hu, S.H. Tian, Y. Xiong, Adsorption performance of hollow spherical sludge carbon prepared from sewage sludge and polystyrene foam wastes, Acs. Sustain. Chem. Eng. 3 (2015) 552–558.

[26] Activated Carbon, Ç. Ferhan (Ed.), Kirk-Othmer Encyclopedia of Chemical Technology, 2014.

[27] Z.T. Yao, A comprehensive review on the applications of coal fly ash, Earth Sci. Rev. 141 (2015) 105–121.

[28] A.S.R. Górny, Exposure to flour dust in the occupational environment, Int. J. Occup. Saf. Ergon. 21 (2015) 241–249.

[29] F.Q. Chen, C.C. Cai, D.G. Cheng, X.L. Zhan, Heat transfer characteristics of alumina membrane coated activated carbon with Core–Shell structure, Ind. Eng. Chem. Res.. 52 (2013) 3653–3657.

[30] D.G. Cheng, W.Y. Jin, X.L. Zhan, F.Q. Chen, Alumina membrane coated activated carbon: a novel strategy to enhance the mechanical properties of a solid catalyst, RSC Adv. 6 (2016) 10229–10232.

[31] Y.K. Lan, T.C. Chen, H.J. Tsai, H.C. Wu, J.H. Lin, I.K. Lin, J.F. Lee, C.S. Chen, Adsorption behavior and mechanism of antibiotic sulfamethoxazole on carboxylic-functionalized carbon nanofibers-encapsulated Ni magnetic nanoparticles, Langmuir 32 (2016) 9530–9539.

[32] J.A. Gao, J.A. Pedersen, Adsorption of sulfonamide antimicrobial agents to clay minerals, Environ. Sci. Technol. 39 (2005) 9509–9516.

[33] L. Nielsen, T.J. Bandosz, Analysis of sulfamethoxazole and trimethoprim adsorption on sewage sludge and fish waste derived adsorbents, Microporous Mesoporous Mater. 220 (2016) 58–72.

[34] J. Li, G.W. Yu, S.Y. Xie, Lj. Pan, C.X. Li, F.T. You, Y. Wang, Immobilization of heavy metals in ceramsite produced from sewage sluge biochar, Sci. Total. Environ.. (2018) 628–629 131-140.

[35] C. Garnero, V. Aiassa, M. Longhi, Sulfamethoxazole: hydroxypropyl-beta-cyclodextrin complex: preparation and characterization, J. Pharm. Biomed. Anal. 63 (2012) 74–79.

[36] M. Ghaedi, F. Karimi, B. Barazesh, R. Sahraei, A. Daneshfar, Removal of reactive Orange 12 from aqueous solutions by adsorption on tin sulfide nanoparticle loaded on activated carbon, J. Ind. Eng. Chem. 19 (2013) 756–763.

[37] Y.Y. Lou, Z.L. Ye, S.H. Chen, Q.S. Wei, J.Q. Zhang, X. Ye, Influences of dissolved organic matters on tetracyclines transport in the process of struvite recovery from swine wastewater, Water Res. 134 (2018) 311–326.

[38] M.S. Ali, M.A.A. Hanim, S.M. Tahir, C.N.A. Jaafar, N. Mazlan, K. Amin Matori, The effect of commercial rice husk Ash additives on the porosity, mechanical properties, and microstructure of alumina ceramics, Adv. Mater. Sci. Eng. (2017) 1–10 2017.

[39] A. Mittal, J. Mittal, A. Malviya, V.K. Gupta, Removal and recovery of chrysoidine Y from aqueous solutions by waste materials, J. Colloid Interf. Sci. 344 (2010) 497–507.

[40] Y.B. Tang, Q. Liu, F.Y. Chen, Preparation and characterization of activated carbon from waste ramulus mori, Chem. Eng. J. 203 (2012) 19–24.

[41] M. Vukcevic, A. Kalijadis, B. Babic, Z. Lausevic, M. Lausevic, Influence of different carbon monolith preparation parameters on pesticide adsorption, J. Serb. Chem. Soc. 78 (2013) 1617–1632.

[42] M. Rundans, I. Sperberga, Porous cordierite ceramics from natural clays /Poraina kordierīta keramika no dabiskiem māliem, Mater. Sci. Appl.Chem. 32 (2015) 33–38.

[43] J.W. Lim, Y. Choi, H.S. Yoon, Y.K. Park, J.H. Yim, J.K. Jeon, Extrusion of honeycomb monoliths employed with activated carbon-LDPE hybrid materials, J. Ind. Eng. Chem. 16 (2010) 51–56.

[44] Z.R. Yue, J. Economy, Synthesis of highly mesoporous carbon pellets from carbon black and polymer binder by chemical activation, Microporous Mesoporous Mater. 96 (2006) 314–320.

[45] R. Wirasnita, T. Hadibarata, A.R.M. Yusoff, Z. Yusop, Removal of bisphenol A from aqueous solution by activated carbon derived from oil Palm empty fruit bunch, Water Air Soil. Poll. 225 (2014).

[46] W.T. Tsai, C.W. Lai, T.Y. Su, Adsorption of bisphenol-A from aqueous solution onto minerals and carbon adsorbents, J. Hazard. Mater. 134 (2006) 169–175.

[47] L.R. Radovic, C. Moreno-Castilla, J. Rivera-Utrilla, Carbon materials as adsorbents in aqueous solutions, Chem. Phys. Carbon. 27 (2001) 227–405.

[48] A.I. Moral-Rodriguez, R. Leyva-Ramos, R. Ocampo-Perez, J. Mendoza-Barron, I.N. Serratos-Alvarez, J.J. Salazar-Rabago, Removal of ronidazole and sulfa-methoxazole from water solutions by adsorption on granular activated carbon: equilibrium and intraparticle diffusion mechanisms, Adsorption. 22 (2016) 89–103.

[49] R. Rostamian, H. Behnejad, A comparative adsorption study of sulfamethoxazole onto graphene and graphene oxide nanosheets through equilibrium, kinetic and thermodynamic modeling, Process Saf. Environ.. 102 (2016) 20–29.

[50] I.B. Toledo, M.A. Ferro-Garcia, J. Rivera-Utrilla, C. Moreno-Castilla, F.J.V. Fernandez, Bisphenol A removal from water by activated carbon. Effects of carbon characteristics and solution chemistry, Environ. Sci. Technol. 39 (2005) 6246–6250.

[51] Y.B. Zhou, L. Chen, P. Lu, X.Y. Tang, J. Lu, Removal of bisphenol A from aqueous solution using modified fibric peat as a novel biosorbent, Sep. Purif. Technol. 81 (2011) 184–190.

[52] R.W. Coughlin, F.S. Ezra, Role of surface acidity in the adsorption of organic pol-lutants on the surface of carbon, Environ. Sci. Technol. 2 (1968) 291–297.

[53] L.D. Nghiem, A.I. Schafer, M. Elimelech, Pharmaceutical retention mechanisms by nanofiltration membranes, Environ. Sci. Technol. 39 (2005) 7698–7705.

[54] D.Q. Zhu, S.H. Hyun, J.J. Pignatello, L.S. Lee, Evidence for π-π electron donor-acceptor interactions between pi-donor aromatic compounds and π-acceptor sites in soil organic matter through pH effects on sorption, Environ. Sci. Technol. 38 (2004) 4361–4368.

[55] D.Q. Zhu, J.J. Pignatello, Characterization of aromatic compound sorptive inter-actions with black carbon (charcoal) assisted by graphite as a model, Environ. Sci.Technol. 39 (2005) 2033–2041.

[56] W. Lertpaitoonpan, S.K. Ong, T.B. Moorman, Effect of organic carbon and pH on soil sorption of sulfamethazine, Chemosphere. 76 (2009) 558–564.

[57] S.W. Nam, C. Jung, H. Li, M. Yu, J.R.V. Flora, L.K. Boateng, N. Her, K.D. Zoh, Y. Yoon, Adsorption characteristics of diclofenac and sulfamethoxazole to graphene oxide in aqueous solution, Chemosphere. 136 (2015) 20–26.

[58] K.L. Chen, L.C. Liu, W.R. Chen, Adsorption of sulfamethoxazole and sulfapyridine antibiotics in high organic content soils, Environ. Pollut. 231 (2017) 1163–1171.

[59] Y. Liu, X.H. Liu, W.P. Dong, L.L. Zhang, Q. Kong, W.L. Wang, Efficient adsorption of sulfamethazine onto modified activated carbon: A plausible adsorption mechanism, Sci. Rep.Uk. 7 (2017) 12–37.

[60] Q. Chen, J.W. Zheng, J.C. Xu, Z. Dang, L.J. Zhang, Insights into sulfamethazine adsorption interfacial interaction mechanism on mesoporous cellulose biochar: coupling DFT/FOT simulations with experiments, Chem. Eng. J. 356 (2019) 341–349.

[61] S. Li, X. Zhang, Y. Huang, Zeolitic imidazolate framework-8 derived nanoporous carbon as an effective and recyclable adsorbent for removal of ciprofloxacin anti-biotics from water, J. Hazard. Mater. 321 (2017) 711–719.